World Academy of Science, Engineering and Technology
International Journal of Electrical and Computer Engineering
Vol:5, No:12, 2011

A Power Conversion System using the Renewable Energies for HEV Charger

Jin-Hong Kim, Joon Sung Park, Jun-Hyuk Choi, and In-Soung Jung

***Abstract*—** With a development of Hybrid Electric Vehicle(HEV), A photovoltaic(PV) generation system is used for charging batteries in many cases. A dc/dc converter using PV power for a battery charger requires a high efficiency. In this paper, A ZVS boost converter using the renewable energies for HEV charger is proposed. Through the theoretical analysis and experimental result, operation modes and characteristics of the proposed topology are verified.

***Keywords*—**HEV, EV, charger, resonant

I. Introduction

An energy crisis has become a global issue due to its scarcity and high rocketing price of fossil energy resources. And CO_2 emission has stabilized and the temperature has increased. For these reasons, renewable energy and Hybrid Electric Vehicle(HEV) have been brought to public attention, and a considerable number of researches have been conducted on these fields[1]. In general, HEV is composed of the battery pack, the traction motor, the inverter and the engine[2]. The capacity of the batteries is one of the determining factors of HEV mileage[3]. So it is important that the battery is charged enough. Therefore, a dc/dc converter is needed for the battery energy storage system. Also, if renewable energy is used for charging the car during the car is parked, the electric charges can be saved.

In this paper, a ZVS boost converter using renewable energies for HEV charger station is proposed. The proposed system contains a Maximum Power Point Tracking(MPPT) algorithm[4] and a Constant Current-Constant Voltage(CC-CV) control method[5]. By using a resonance circuit, the proposed topology can reduce the switching loss because the switch is turned on and off with zero voltage switching (ZVS). The proposed topology is verified through simulation and experimental results.

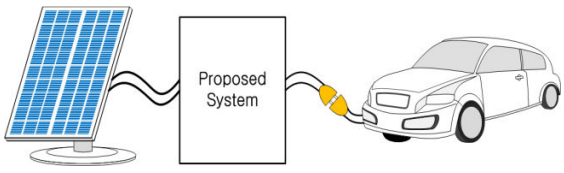

Fig. 1 A schematic of the proposed system

Jin-Hong Kim , Joon Sung Park, Jun-Hyuk Choi, and In-Soung Jung are with the Korea Electronics Technology Institute, 203-101 Bucheon-TP B/D, Yakdae-dong, Wonmi-gu, Bucheon-si, Gyeonggi-do, Korea, 420-140 (e-mail: kimjinhong@keti.re.kr)

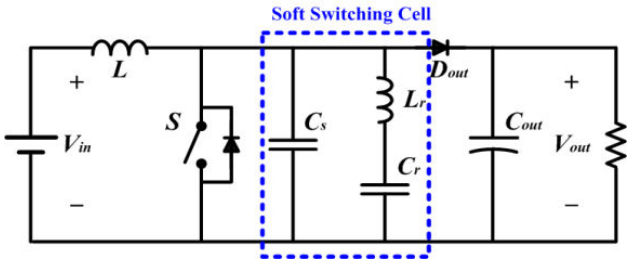

Fig. 2 A schematic of the proposed converter

II. Proposed Soft Switching Boost Converter

A. Composition of proposed converter

Fig. 1 shows a schematic of the proposed system. The proposed system transfers a DC power from PV array to batteries of a HEV.

Fig. 2 shows a schematic of the proposed a soft switching boost converter using the PV power for HEV charger station. The proposed converter is based on a conventional boost converter with a soft switching cell that consists of a resonant inductor L_r, a resonant capacitor C_r and a snubber capacitor C_s.

B. Operation mode

In this section, an operating mode analysis of the proposed converter is performed according to the different current paths of each elements and the voltage of the switch. The proposed topology is divided into 7 modes. Fig. 3 shows the key waveforms of the proposed converter during a single switching period. Fig. 4 shows the operation modes.

Mode 1 ***($t_0 \le t < t_1$)*** : Mode 1 starts when the switch is turned on. The main inductor current(i_L) flows to switch and resonant circuit. During this mode, the resonant inductor current(i_{Lr}) decreases to zero. When the resonant capacitor (Cr) is full charged, Mode 1 is finished.

$$i_{Lr}(t) = i_L(t_0)\cos\omega_r t - \frac{v_{Cr}(t_0)}{Z_r}\sin\omega_r t \quad (1)$$

$$v_{Cr}(t) = v_{Cr}(t_0)\cdot\cos\omega_r t + i_L(t_0)\cdot Z_r \sin\omega_r t \quad (2)$$

Where the characteristic impedance(Z_r) and the resonant angular frequency (ω_r) are defined in Eq. (3)

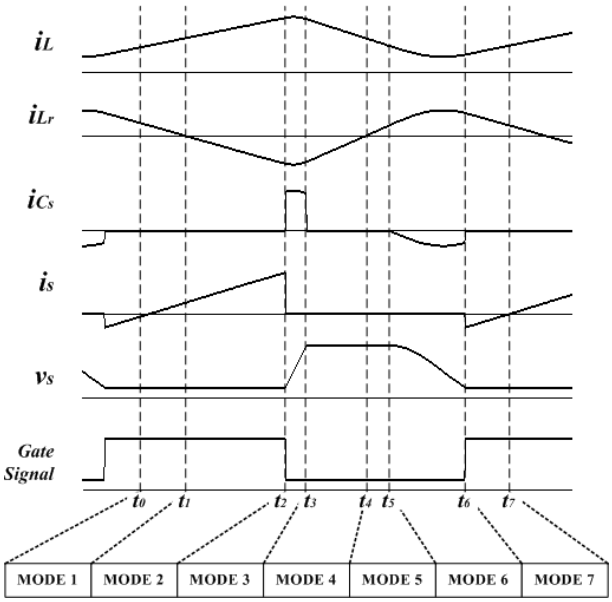

Fig. 3 Key waveforms of the proposed converter

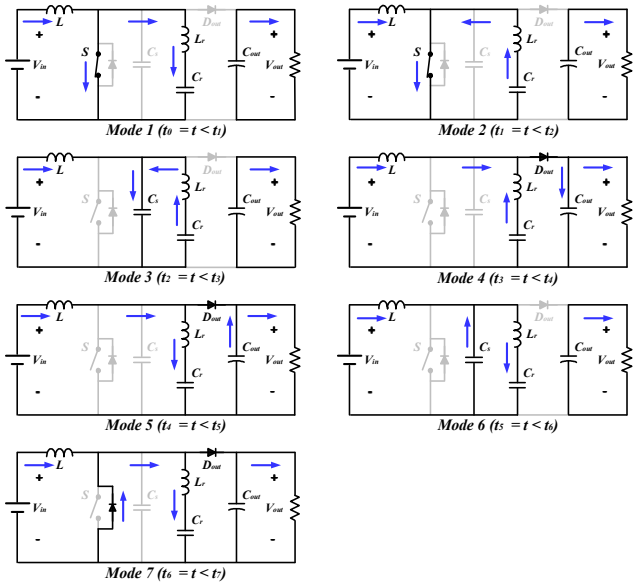

Fig. 4 Operation modes of proposed converter

$$\omega_r = \frac{1}{Z_r},\ Z_r = \sqrt{L_r \cdot C_r}\ . \tag{3}$$

Mode 2 ***($t_1 \le t < t_2$)*** : At time t_1, the direction of i_{Lr} is changed. i_L and i_{Lr} are added together and the resulting current flows to the switch.

$$i_{Lr}(t) = -\frac{v_{Cr}(t_1)}{Z_r}\sin\omega_r t \tag{4}$$

$$v_{Cr}(t) = v_{Cr}(t_1)\cdot\cos\omega_r t \tag{5}$$

Mode 3 ***($t_2 \le t < t_3$)*** : This mode is started when the switch S is turned off with ZVS condition, due to the snubber capacitor(*Cs*). i_L and i_{Lr} flows to C_s together and C_s is charged. When *Cs* is full charged, mode 3 ends.

$$i_{Lr}(t) = \frac{C}{C_s}i_L(t_2) + \left(i_{Lr}(t_2) - \frac{C}{C_s}i_L(t_2)\right)\cos\omega_a t - \frac{v_{Cr}(t_2)}{Z_a}\sin\omega_a t \tag{6}$$

$$v_{Cr}(t) = \frac{i_L(t_2)}{C_r + C_s}t + \frac{C}{C_s}\cdot v_{Cr}(t_2)\cdot\left(1 + \frac{C_s}{C_r}\cos\omega_a t\right) + \frac{C}{C_r}Z_a\left(i_{Lr}(t_2) - \frac{C}{C_s}i_L(t_2)\right)\sin\omega_a t \tag{7}$$

$$v_{Cs}(t) = \frac{i_L(t_2)}{C_r + C_s}t + \frac{C}{C_s}\cdot v_{Cr}(t_2)\cdot(1 - \cos\omega_a t) + \frac{C}{C_s}Z_a\left(\frac{C}{C_s}i_L(t_2) - i_{Lr}(t_2)\right)\sin\omega_a t \tag{8}$$

where $\omega_a = \frac{1}{\sqrt{L_r C}},\ Z_a = \sqrt{\frac{L_r}{C}},\ C = \frac{C_r C_s}{C_r + C_s}$.

Mode 4 ***($t_3 \le t < t_4$)*** : At time t_3, the voltage across *Cs* is equal to output voltage (*Vout*) and output diode (*Dout*) begins to conduct. The saved energy of the main inductor (*L*) and the resonant circuit are transmitted to the load through *Dout*. Mode 4 ends when *Cr* is fully discharged and the direction of i_{Lr} is changed.

$$i_{Lr}(t) = i_{Lr}(t_3)\cdot\cos\omega_r t + \frac{V_o - v_{Cr}(t_3)}{Z_r}\sin\omega_r t \tag{9}$$

$$v_{Cr}(t) = V_o - (V_o - v_{Cr}(t_3))\cos\omega_r t + i_{Lr}(t_3)\cdot Z_r\sin\omega_r t \tag{10}$$

Mode 5 ***($t_4 \le t < t_5$)*** : i_L flows to the resonant circuit and the load. i_{Lr} changes the direction. When i_L has become equal to i_{Lr}, this mode is finished.

$$i_{Lr}(t) = \frac{V_o - v_{Cr}(t_4)}{Z_r}\sin\omega_r t \tag{11}$$

$$v_{Cr}(t) = V_o - (V_o - v_{Cr}(t_4))\cdot\cos\omega_r t \tag{12}$$

Mode 6 ***($t_5 \le t < t_6$)*** : Mode 6 starts with discharging of *Cs*. When the voltage across *Cs* becomes lower than *Vout*, *Dout* turns off and mode 6 ends.

$$i_{Lr}(t) = \frac{C}{C_s} i_L(t_5)(1+\frac{C_s}{C_r}\cos\omega_a t) + \frac{V_o - v_{Cr}(t_5)}{Z_a}\sin\omega_a t \quad (13)$$

$$v_{Cr}(t) = \frac{I_L(t_5)}{C_r + C_s} t + v_{Cr}(t_5) + \frac{C}{C_r}(V_o - v_{Cr}(t_5))(1-\cos\omega_a t) + \left(\frac{C}{C_r}\right)^2 i_L(t_5) Z_a \sin\omega_a t \quad (14)$$

$$v_{Cs}(t) = \frac{i_L(t_5)}{C_r + C_s} t + \frac{C}{C_r} V_o (1+\frac{C_r}{C_s}\cos\omega_a t) + \frac{C}{C_s}\cdot v_{Cr}(t_5)\cdot(1-\cos\omega_a t) - \frac{C}{C_r + C_s} i_L(t_5) Z_a \sin\omega_a t \quad (15)$$

when $C = \frac{C_r C_s}{C_r + C_s}$, $Z_a = \sqrt{\frac{L_r}{C}}$, $\omega_a = \frac{1}{\sqrt{L_r C}}$.

Mode 7 ***($t_6 \le t < t_7$)*** : When i_{Lr} flows to switch's parallel diode with full discharging of *Cs*, this mode starts. The switch *S* is turned on with ZVS condition. When switch's parallel diode turns off, mode 7 ends.

$$i_{Lr}(t) = i_{Lr}(t_6)\cos\omega_r t - \frac{v_{Cr}(t_6)}{Z_r}\sin\omega_r t \quad (16)$$

$$v_{Cr}(t) = v_{Cr}(t_6)\cdot\cos\omega_r t + i_{Lr}(t_6)\cdot Z_r \sin\omega_r t \quad (17)$$

III. Simulation

A computer simulation for operational characteristics of proposed dc/dc converter was executed by using PSIM software. The simulation parameters are shown in Table. I. Fig. 5 shows the gate signal, current waveforms, and voltage waveforms of the proposed converter when the input voltage is 80[V]. The output voltage is controlled to DC 400[V].

Fig. 6 shows current and voltage of switch *S* and Gate signal. The proposed converter is able to perform a ZVS. So it is expected that efficiency of proposed converter is higher than that of a conventional boost converter.

Fig. 7 shows control blocks of proposed system. The proposed system requires a MPPT control for an input power and a CC-CV control for an output power. If control signals of two control methods are mutually exclusive, a CC-CV control is must be a priority factor.

TABLE I
SIMULATION PARAMETERS

Parameter	Value
Main inductor *L*	500 [μH]
Resonant inductor *Lr*	100 [μH]
Snubber capacitor *Cs*	60 [nF]
Resonant capacitor *Cr*	2600 [nF]
Output capacitor *Cout*	500 [μF]
Input voltage	80 [V]
Output voltage	400 [V]
Power	400 [W]

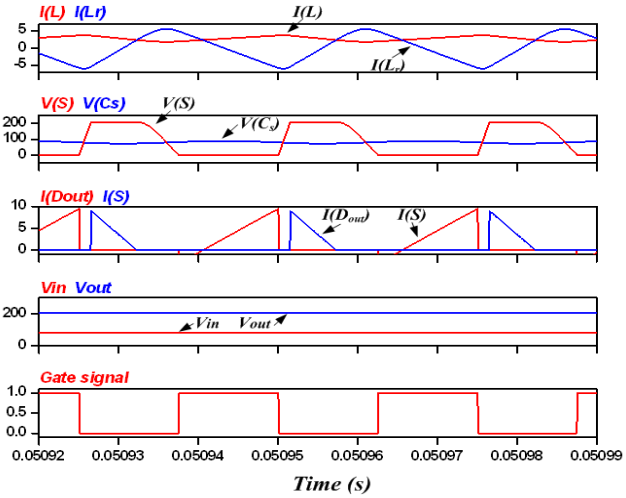

Fig. 5 Current waveforms, voltage waveforms and gate signal of the proposed converter

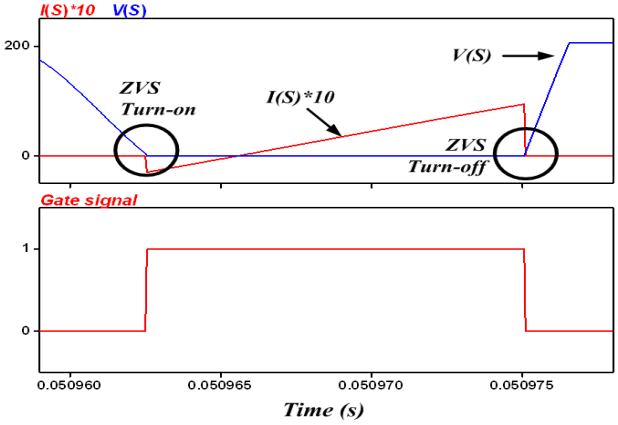

Fig. 6 Current and voltage of switch S

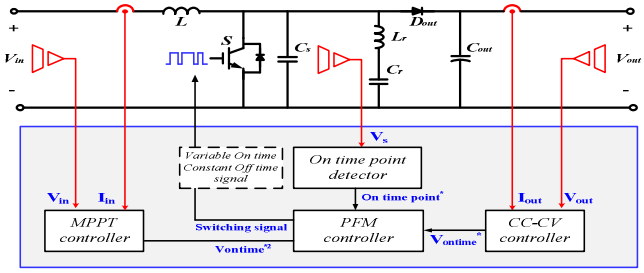

Fig. 7 Control blocks of proposed system

TABLE II
SPECIFICATIONS OF PROPOSED CONVERTER

Parameter	Value
Main inductor *L*	504.2 [μH]
Resonant inductor *Lr*	101.2 [μH]
Switch *S*	IXSX40N60BD1
Output diode *Dout*	F40U60DN
Snubber capacitor *Cs*	66 [nF]
Resonant capacitor *Cr*	2660 [nF]
Output capacitor *Cout*	500 F]

IV. EXPERIMENTAL RESULT

Experiments were conducted on a 400 [W] to verify the analysis and simulation results. The parameters used in the experimental system are given in Table. II.

Fig. 8 shows resonant inductor current, switch and resonant capacitor voltage waveforms. The proposed boost converter performs ZVS when switch is turned on and off. Fig. 9 shows resonant inductor current, output and input voltage waveforms.

V. CONCLUSION

In this paper, a soft switching boost converter using the PV power for HEV charger station is proposed. The proposed topology is verified through simulation and experimental results. The proposed topology performs ZVS when the switch is turned on and off.The proposed topology can deliver renewable energies to batteries with high efficiency. So it is expected that the proposed topology makes renewable energies more useful.

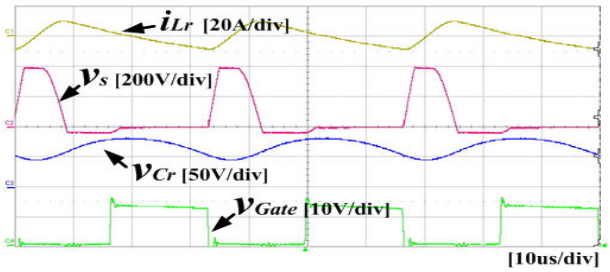

Fig. 8 Resonant Inductor current, switch and resonant capacitor voltage Waveforms

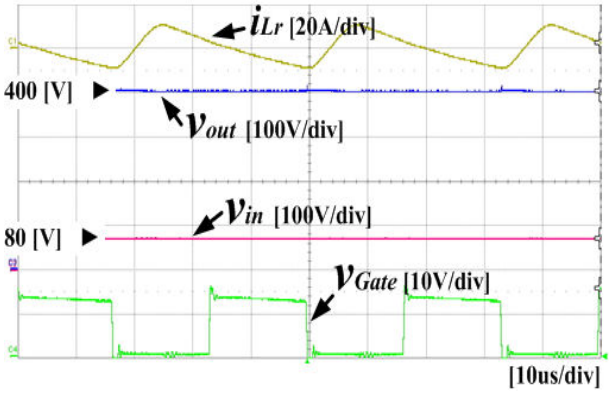

Fig. 9 Resonant Inductor current, output and input voltage Waveforms

REFERENCES

[1] C. C. Chan, "The state of the art of electric, hybrid, and fuel cell vehicles," *Proceedings Of The Ieee*, vol. 95, no. 4, pp. 704–718, Apr. 2007.

[2] T. Bradley and A. Frank, "Design, demonstrations and sustainability impact assessments for plug-in hybrid electric vehicles," *Renewable Sustainable Energy Rev*, vol. 13, no. 1, pp. 115–128, 2009.

[3] B. Sovacool and R. Hirsh, "Beyond batteries: An examination of the benefits and barriers to plug-in hybrid electric vehicles (phevs) and a vehicle-to-grid (v2g) transition," *Energy Policy*, vol. 37, no. 3, pp. 1095–1103, 2009.

[4] Y.C. Kuo, T.J. Liang, and J.F. Chen, "Novel Maximum-Power-Point-Tracking Controller for Photovoltaic Energy Conversion System," IEEE Trans. on Industrial Electronics, Vol. 48, No. 3, pp. 594-601, 2001, Jun.

[5] S. Jung, Y.Woo, N. Kim, and G. Cho, "Analog-digital switching mixed mode low ripple—high efficiency Li-Ion battery charger," in *Proc. Ind.Appl. Conf.*, 2001, vol. 4, pp. 2473–2477.